The difference in the composite of surge elevation and wave height for respective scenarios is presented in Figure 24. The vast majority of the study site underwent a considerable increase in SEWH values. The maximum difference occurs along the east flank of East Island showing an increase of 32 ft. This value is high because the east flank of the island migrated westward and land was transformed into water over the approximate 40 year period. Notably, the largest increases occur along the bay shorelines and barriers proper where land was transformed into water during the intervening time period. Where water was transformed into land through barrier migration, a reduction in SEWH is observed. The magnitude of increase is typically 8-10 ft although change >12 ft is readily apparent along the marsh shorelines and barriers.

Change in Surge and Wave Height: Early1990's – 2020

As presented in Figure 25, changes in maximum storm surge elevation over this approximate 30 year period appear as a significant increase throughout much of the study site. The largest change occurs along the barrier coast and bay fringing marsh north of Isles Dernieres where increases of between 10 and greater than 12 ft were computed. In the marshes flanking Terrebonne Bay increases typically range from 1 to 6 ft, with a few locations showing 10 ft. The highest increase of 33 ft was computed at Fourchon.

Change in maximum significant wave height is presented in Figure 26. With a maximum increase of 13 ft occurring at Fourchon, the remainder of the study area shows a large percentage of increase throughout. Increases of up to 5 ft occur along the Isles Dernieres and bay marsh shoreline to the north. Six to 8 ft increases occurred along Timbalier Island. In the marsh north of Terrebonne Bay, wave height increased between 1 and 4 ft.

The composite of maximum surge and wave height differences is presented in Figure 27. The increase in SEWH is widespread in the study area with the largest increases occurring at Fourchon (45 ft), Timbaliers and in particular, Isles Dernieres and the adjacent marshes. At these locations increasing values of SEWH range from 10 to >12 ft. Throughout the marsh north of Terrebonne Bay, values increase from 6 ft, although in several location increases between 10 and >12 ft were computed.

Change in Surge and Wave Height: 1950 – 2020

Changes in surge, wave height and the composite of both are presented in Figures 28, 29 and 30 for the 70 year period between 1950 and 2020. The trends are, as expected, similar to those discussed for the two time scenario presented earlier in this report. What is clearly evident from all figures and particularly the composite image in Figure 30, is that almost the entire study area experiences a significant increase in storm surge and wave inundation for the 70 year time difference. Virtually the entire barrier coast experiences an increase greater than 12 ft as does most of the fringing bay marsh. The interior of the marsh experiences typically 6-8 ft increases, although isolated areas experiencing > 12 ft also occur.

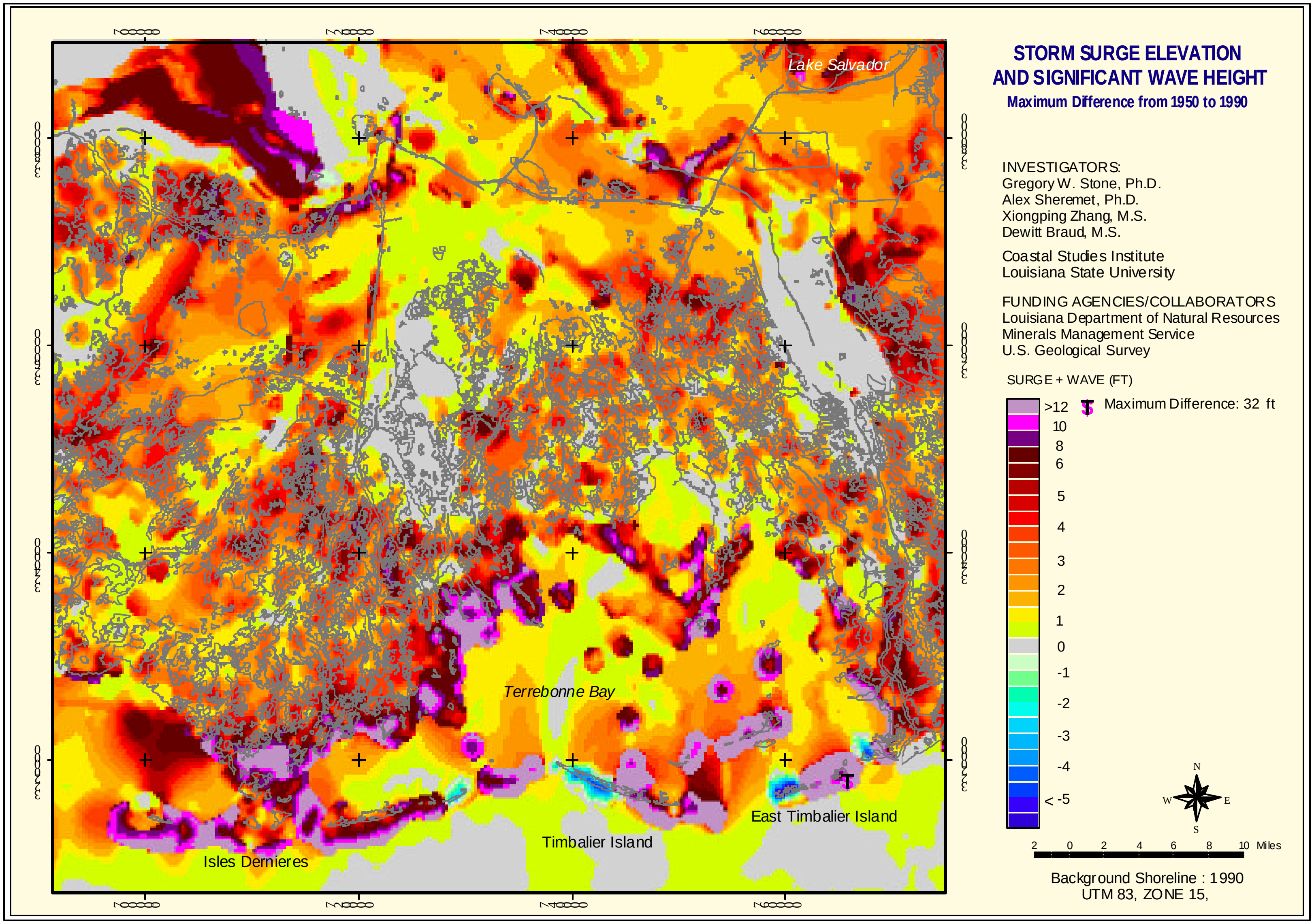

Figure 24. Difference in Maximum Storm Surge and Significant Wave Height between 1950 and 1990's scenarios.

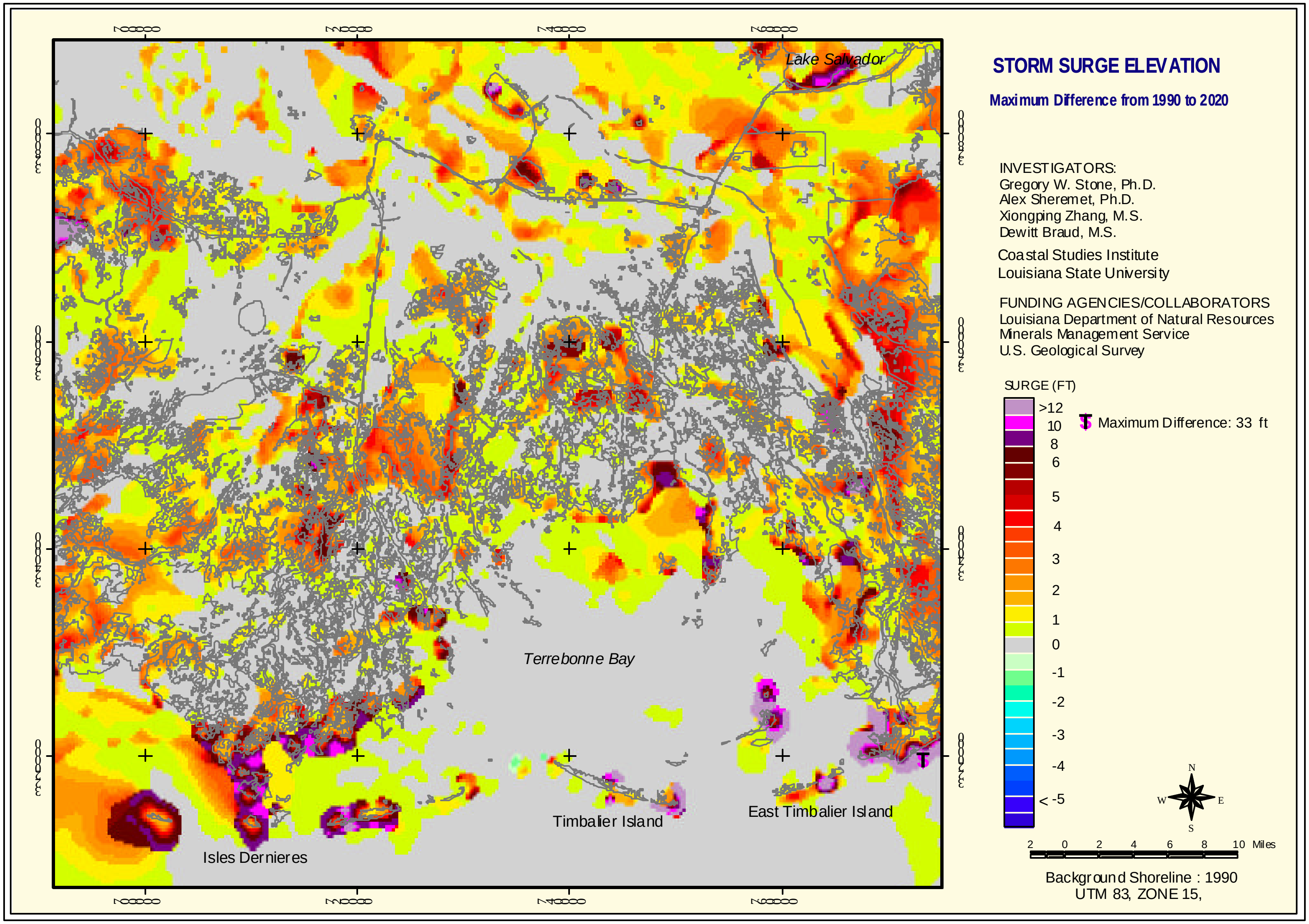

Figure 25. Difference in Maximum Storm Surge between 1990's and 2020 scenarios.

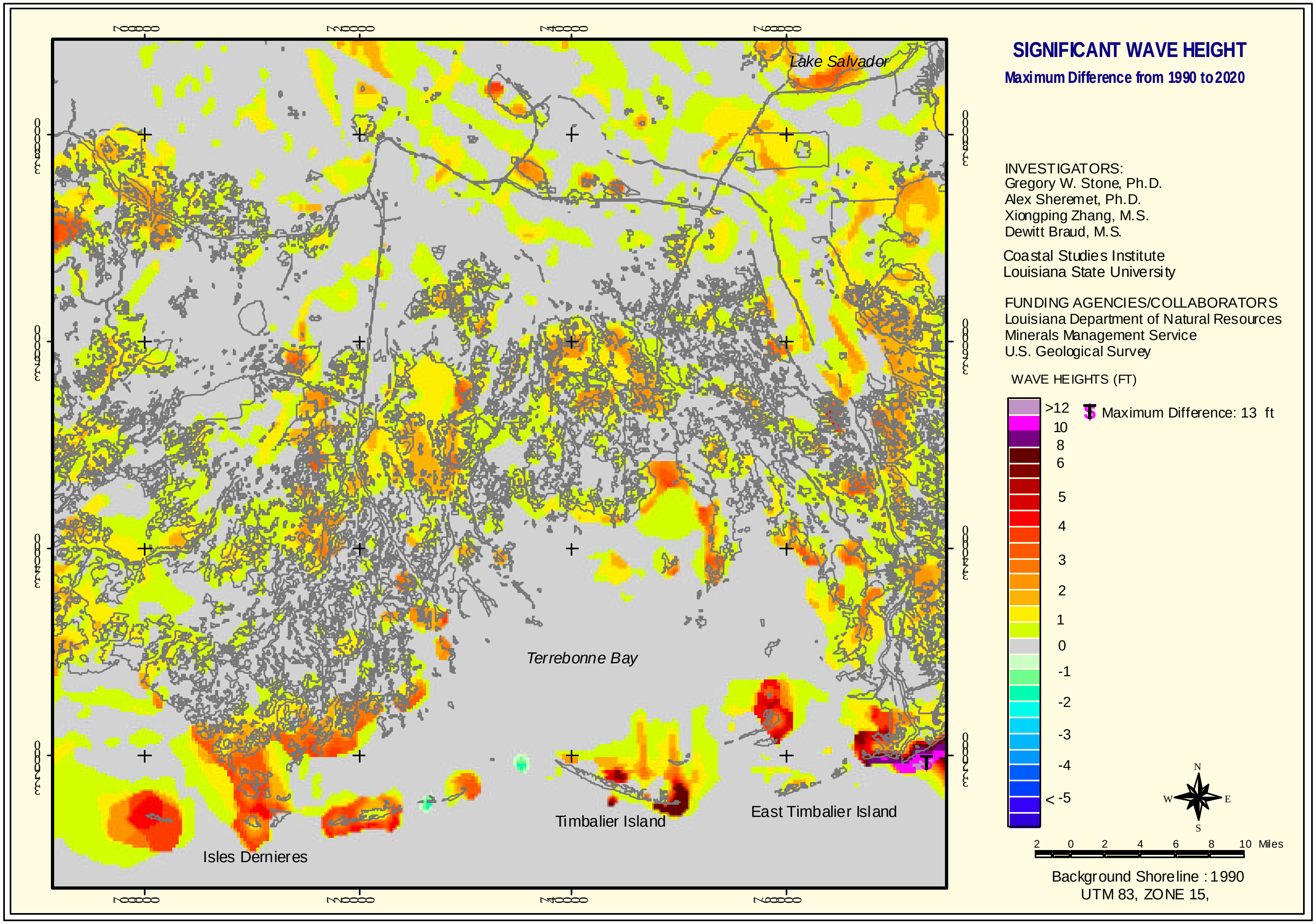

Figure 26. Difference in Maximum Significant Wave Height between 1990's and 2020 scenarios.

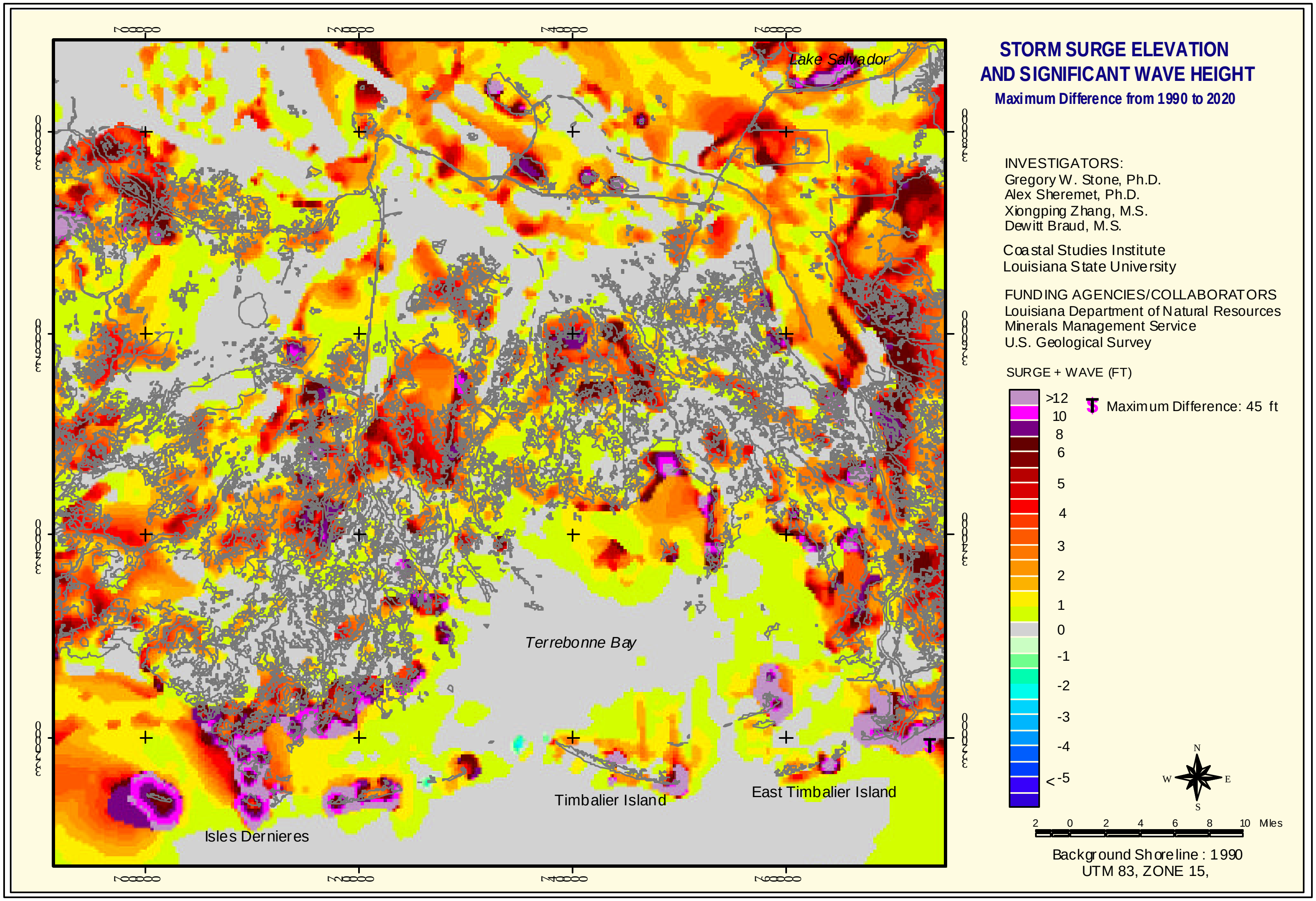

Figure 27. Difference in Maximum Storm Surge and Maximum Wave Height between 1990's and 2020 scenarios.

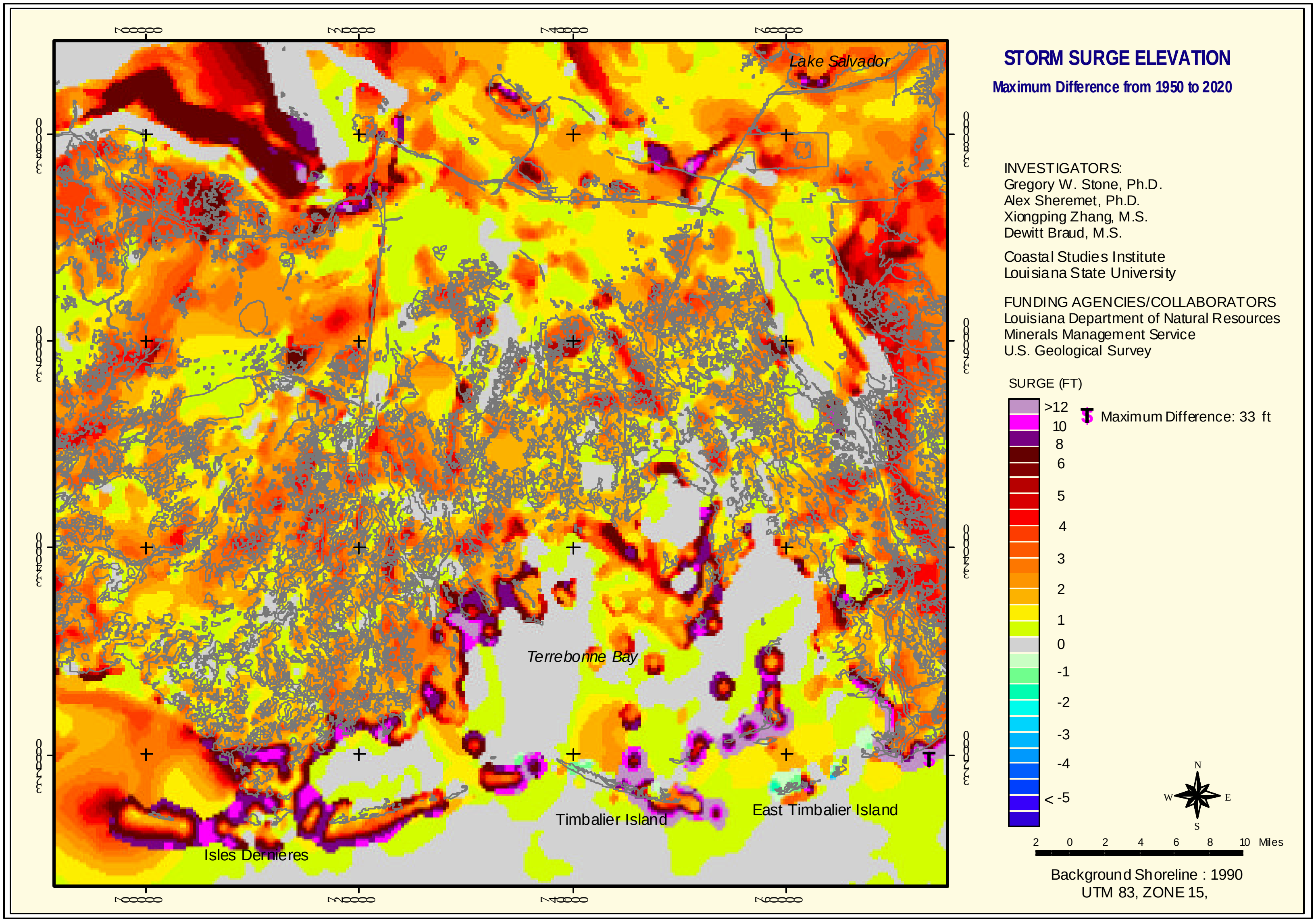

Figure 28. Difference in Maximum Storm Surge between 1950 and 2020 scenarios.

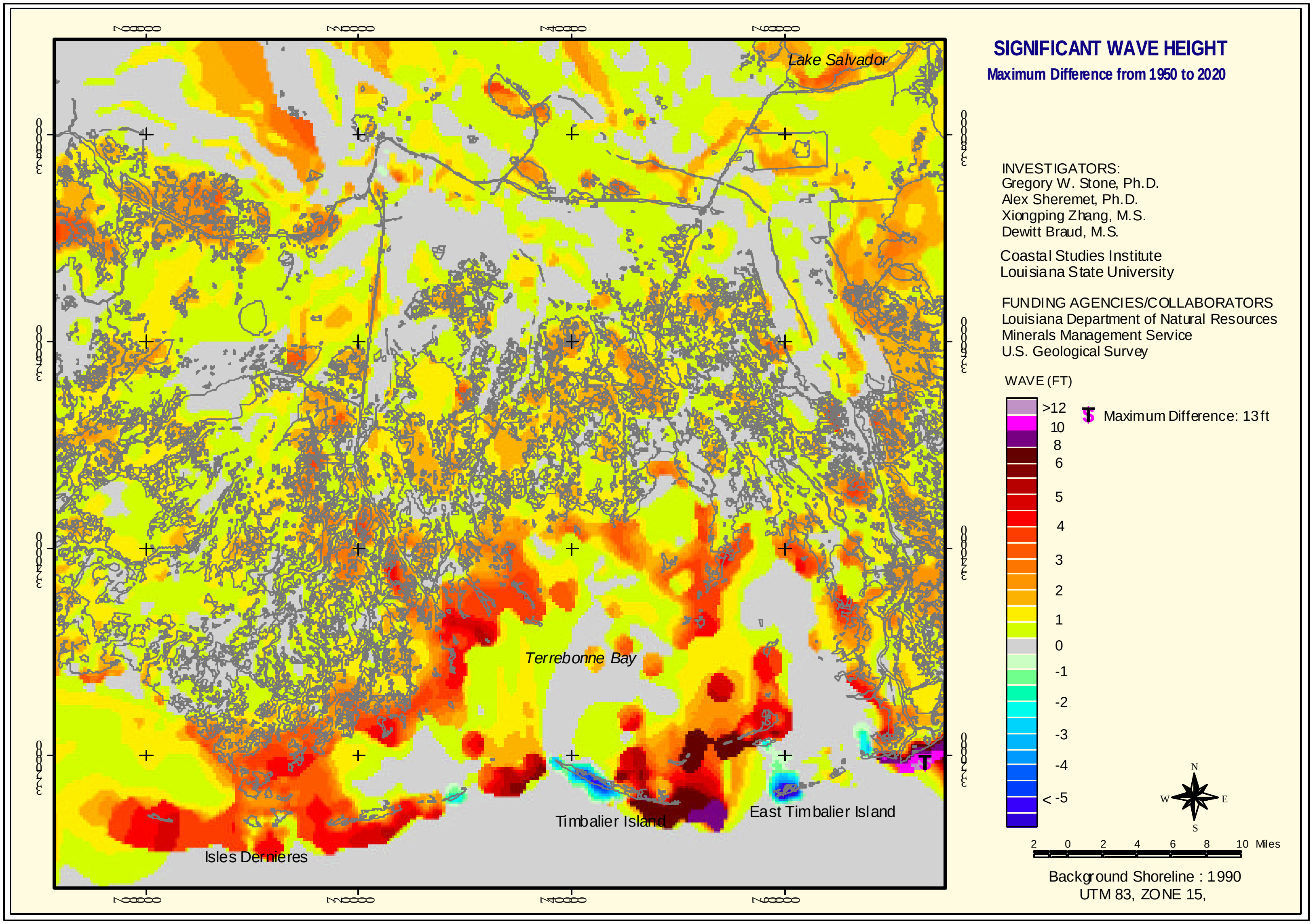

Figure 29. Difference in Maximum Significant Wave Height between 1950 and 2020 scenarios.

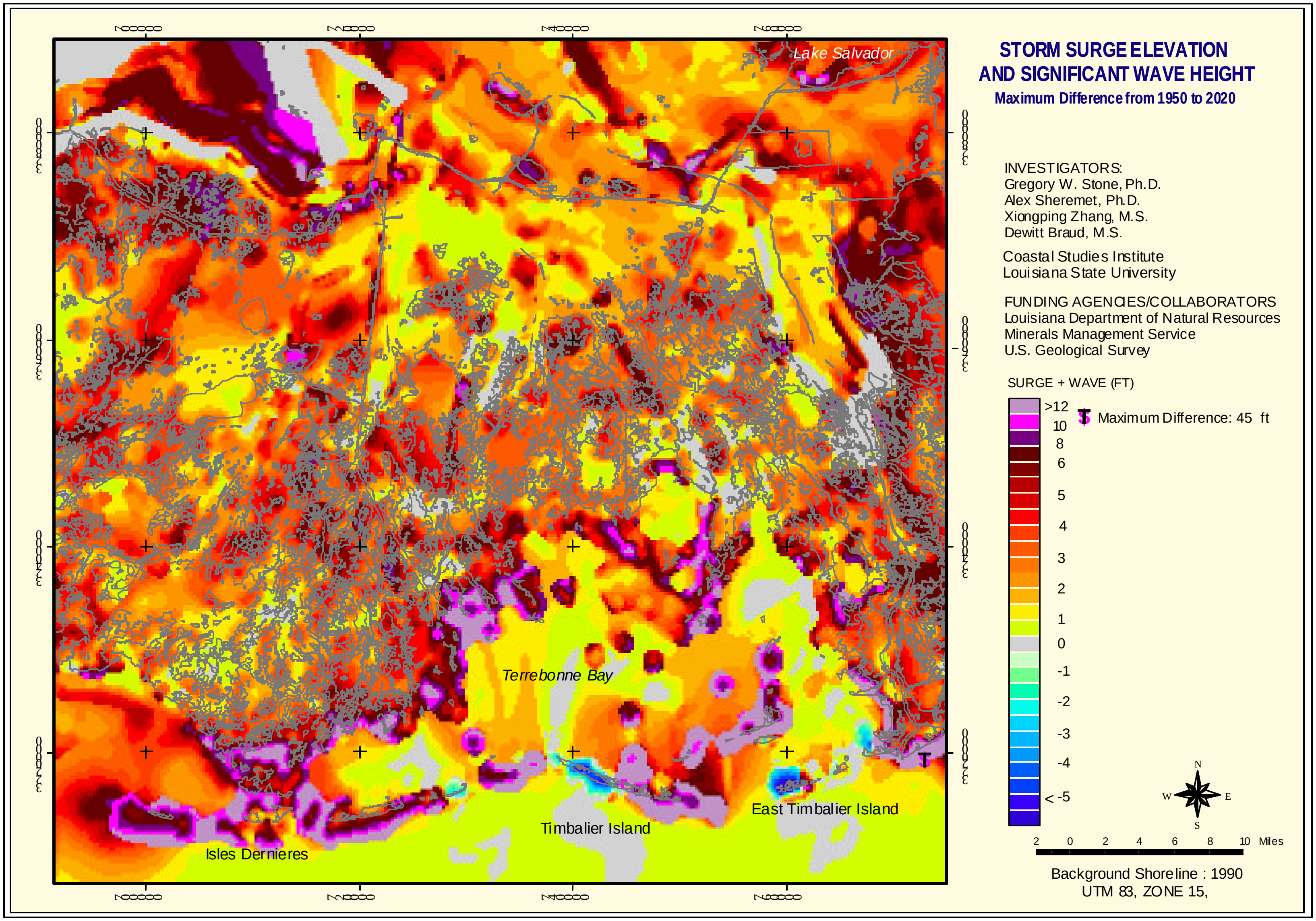

Figure 30. Difference in Maximum Storm Surge and Maximum Wave Height between 1950 and 2020 scenarios.

Degree of Surface Area Inundation

It is clearly evident from the comparisons of both surge and wave height presented here that physical loss of the barrier islands and marsh resulted in a considerable increase in modeled surge levels and wave heights. It is also notable that while this response is clearly evident on the barrier coast, the composite of waves and surge show considerably more inundation for the 1990's scenario when compared to that of 1950 along the bay marsh shorelines and farther inland. The forecasted erosion of both barriers and marsh to the year 2020 also supports this conclusion. In Figure 31 the degree of surface area inundated is presented for both time intervals. In Figure 31A the area of inundation is plotted against the maximum surge elevation for both time periods. Considering the 1950-1990's scenario, where the curve is above zero, this indicates an increase in area impacted by storm surge. Since storm surge is not uniform throughout the study area, incremental surge levels are plotted against acreage inundated. Change associated with surge levels greater than 15 ft were negligible and not included.

As an example, between 1950 and the early 1990's the acreage impacted by a modeled 7 ft surge increased to 69,000 acres. Similarly, the early 1990's scenario suggests that the acreage impacted by 12 ft surge levels increased to 49,000 acres. When presented in this fashion it is readily apparent that on comparing maximum storm surge levels for both scenarios, the loss of barrier islands and marsh results in an increase in maximum surge levels in the study area. For the 1990's-2020 comparison (Figure 31A) much of the curve shows an increase in acreage to a maximum of 20,000 acres up to the 12 ft surge level. The 12 and 13 ft surge intervals show a decrease of acreage of up to 15,000 acres (12 ft). It is evident, however, that the vast majority of the study area experienced an increase in the surface area inundated by storm surge.

A similar analysis was performed for significant wave height (Figure 31B) and the composite of surge and wave height (Figure 31C). The curve representing significant wave height change and corresponding surface area shows a distinct increase when the 1950 and 1990's scenarios are compared. A peak of 110,000 acres increase corresponds to a wave height of 6 ft. Similarly, comparison of the 1990's and 2020 scenarios show a similar curve, although the peak increase in inundation is less at 58,000 acres. Finally, the composite of maximum surge and significant wave height illustrate the same trend for both scenarios where virtually all of both curves indicate a distinct increase in area inundated increasing to a maximum of slightly greater than 80,000 acres for the 1950-1990's scenario comparisons and 35,000 acres for the 1990's-2020 comparisons.

The data presented in Figure 31A, B and C are based on change that occurred between the respective time intervals, 40 and approximately 30 years. In order to normalize the data for this time discrepancy the data were expressed as a rate of change per year. This was undertaken to remove the differential time bias and the data are presented in Figure 31 D, E and F. While the curves take on exactly the same shape, normalizing for the time disparity reduces the difference in magnitude of the surface area change.

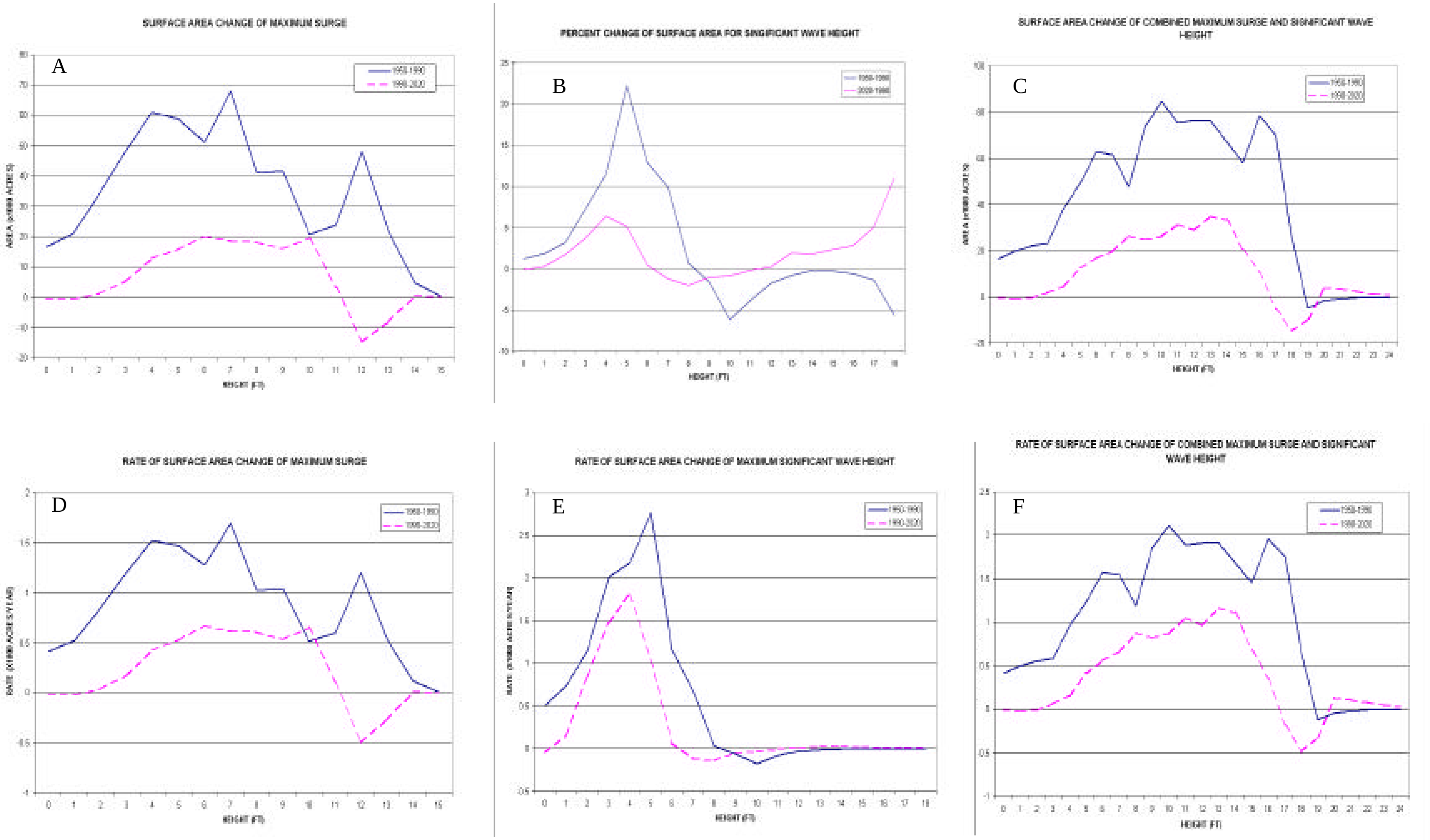

Figure 31. Surface area change of maximum surge (A), maximum significant wave height (B) and the composite of surge and wave height (C). Rate of surface area change of maximum surge (D), maximum significant wave height (E) and the composite of surge and wave height (F).

Geo-Spatial Analysis

The potential impact of hurricanes from storm surge and waves on the oil and gas infrastructure in the study area is enormous due to the extent and number of facilities located there, and to the fact that barrier islands and marshes have drastically diminished in the past 40 years. To illustrate the facilities at risk, the maximum combined surge plus wave height occurring during the entire model sequence for 1990 was captured for each cell. A single layer was created of maximum surge/wave height occurrence, which was used to overlay selected oil and gas facilities located in the study region. GIS geospatial functions were employed to calculate the number or length of oil and gas facilities at risk. These were enumerated and sorted by maximum surge plus wave height. The same procedures were also utilized to tabulate and sort features by the difference in maximum surge plus wave height between 1950 and 2020 based on the model results. The results of these calculations are shown in Tables 1 and 2. The resources at risk were derived from the geospatial layers described below. Table 1 captures the number of facilities at risk as a function of combined maximum surge plus wave height, and illustrates that for each category of resource at risk. The majority of facilities are within the range of 10-20 feet, with a very small percentage falling in higher ranges. The percentage area for each height value is also provided in Table 1, and shows that the 10-19 feet range height accounts for the majority of the study area, so that the pattern that is noted in the table is expected. The majority of facilities would be exposed to very large combined wave and surge heights. Table 2 illustrates the difference in combined maximum surge plus wave height between 1950 and 2020. The percentage area of differences is more even than for the map of maximums, although the differences are more spatially clustered. Nevertheless the resources at risk tend to aggregate in relation to the height areas and do not show a distinct pattern. The table does easily reveal however, that by far, a high percentage of facilities are exposed to larger combined surge plus wave heights.

Petroleum Product Storage Stations and Terminals from LDEQ EIS source data

As presented in Figure 32, this is a data set of point emission sources of volatiles from operations that have Standard Industrial Classification (SIC) codes 4226 or 5171. SIC code 4226 is for 'Special Warehousing and Storage.' This category includes petroleum and chemical bulk stations and terminals for hire. SIC Code 5171 is for 'Petroleum Bulk stations and Terminals.' These are establishments primarily engaged in the wholesale distribution of crude petroleum and petroleum products, including liquefied petroleum gas, from bulk liquid storage facilities. These data were derived from Louisiana Department of Environmental Quality (LDEQ) Emission Inventory System (EIS) source data. There are 7 in the entire study area.

Natural Gas Production and Distribution Facilities

Presented also in Figure 32, is a subset of a point data set from the Equifax Standard Industrial Classification Code (SIC) coded businesses in Louisiana for the locations of all Natural Gas Production and Distribution Facilities having SIC Code 492500. Information includes the business name, addresses, and a contact person with phone number.

Table 1. Oil and gas resources at risk, 1990 maximum surge plus wave height.

Max Surge + Wave Height	Oil & Gas Wells	Crude Petroleum Production Facilities	Natural Gas Production Facilities	Oil & Gas Structures	Percent Area
5	6	0	0	0	0.89%
6	98	0	1	0	3.38%
7	160	33	0	1	2.20%
8	284	0	0	1	2.28%
9	214	0	0	1	2.53%
10	378	37	0	16	5.65%
11	905	98	1	22	6.83%
12	898	60	0	35	7.79%
13	1050	153	0	67	11.85%
14	902	41	2	73	7.09%
15	1361	84	0	89	9.68%
16	1183	68	0	103	11.93%
17	1244	95	1	136	6.78%
18	1297	60	0	188	8.40%
19	1391	50	0	69	4.69%
20	413	144	0	14	2.21%
21	23	0	0	11	1.65%
22	55	0	0	40	1.75%
23	56	0	0	66	1.35%
24	0	0	0	0	0.88%
25	0	0	0	0	0.20%
Totals	**11918**	**923**	**5**	**932**	**100.00%**

Table 2. Oil and gas resources at risk, 1950-2020 maximum surge plus wave height difference.

Difference Max Surge + Wave Height	Oil & Gas Wells	Crude Petroleum Production Facilities	Natural Gas Production Facilities	Oil & Gas Structures	Percent Area
<=0	1572	97	2	314	15.11%
1	1994	178	2	239	18.38%
2	2363	142	2	154	17.54%
3	2133	112	0	78	16.59%
4	1425	64	1	32	11.27%
5	707	28	0	33	6.78%
>=6	2144	334	1	82	14.34%
Totals	**12338**	**955**	**8**	**932**	**100.00%**

Crude Petroleum and Natural Gas Production and Extraction Operations from LDEQ EIS source data

Because of the horizontal spatial resolution of the source data, it is possible for several different NEDS points to fall in the same location in these data, even though they are physically separated at the facility. Furthermore, because individual NEDS points may have several Source Classification Codes, these multiple codes can also result in multiple points at the same location. This is a data set of point emission sources of volatiles from operations that have Standard Industrial Classification (SIC) code 1311, Crude Petroleum and Natural Gas (Extraction) and is presented in Figure 32. This SIC classification includes establishments primarily engaged in operating oil and gas field properties. Such activities may include exploration for crude petroleum and natural gas; drilling, completing, and equipping wells; operation of separators, emulsion breakers, desilting equipment, and field gathering lines for crude petroleum; and all other activities in the preparation of oil and gas up to the point of shipment from the producing property. This industry includes the production of oil through the mining and extraction of oil from oil shale and oil sands and the production of gas and hydrocarbon liquids through gasification, liquid faction, and pyrolysis of coal at the mine site. Also included are establishments which have complete responsibility for operating oil and gas wells for others on a contract or fee basis. These data were derived from Louisiana Department of Environmental Quality (LDEQ) Emission Inventory System (EIS) source data.

Oil and Gas Well Locations, Current Record Version 04/07/1999, Louisiana Department of Natural Resources, Office of Conservation

Presented in Figure 33 is a point dataset of the location of over 160,000 oil and gas wells in the state of Louisiana. It was developed from a database of the permitted and drilled oil and gas wells in the state of Louisiana compiled since the industry was first regulated in the early 1900's. Specifically, the dataset contains the current record (last update to the record) for all of the wells permitted and drilled in Louisiana. These records were obtained from the Office of Conservation legacy database then imported into Oracle and exported to .dbf format to facilitate ArcView operation for in-house and public access GIS. When the department completes its conversion to Oracle, more direct access to the entire historical database for oil and gas wells, including production records and imaged documents) will be made available and linked through various software and hardware configurations, including SDE (ESRI's Spatial Database Engine) for GIS use as well as the department's SONRIS 2000 web access. Numerous data fields for the wells are included in the attribute table.

Oil and Gas Platform Structures in the Gulf of Mexico from MMS source data

This is a point data set for the location of over 4,300 MMS administered platform structures used for oil and gas production in the Gulf of Mexico (Figure 34). Groups of platform structures connected by walkways form 'complexes.' There are approximately 3,700 such complexes in these data. Attribute data including presence of a heliport, number of beds, storage tank presence, and ownership aggregated to the complex level is

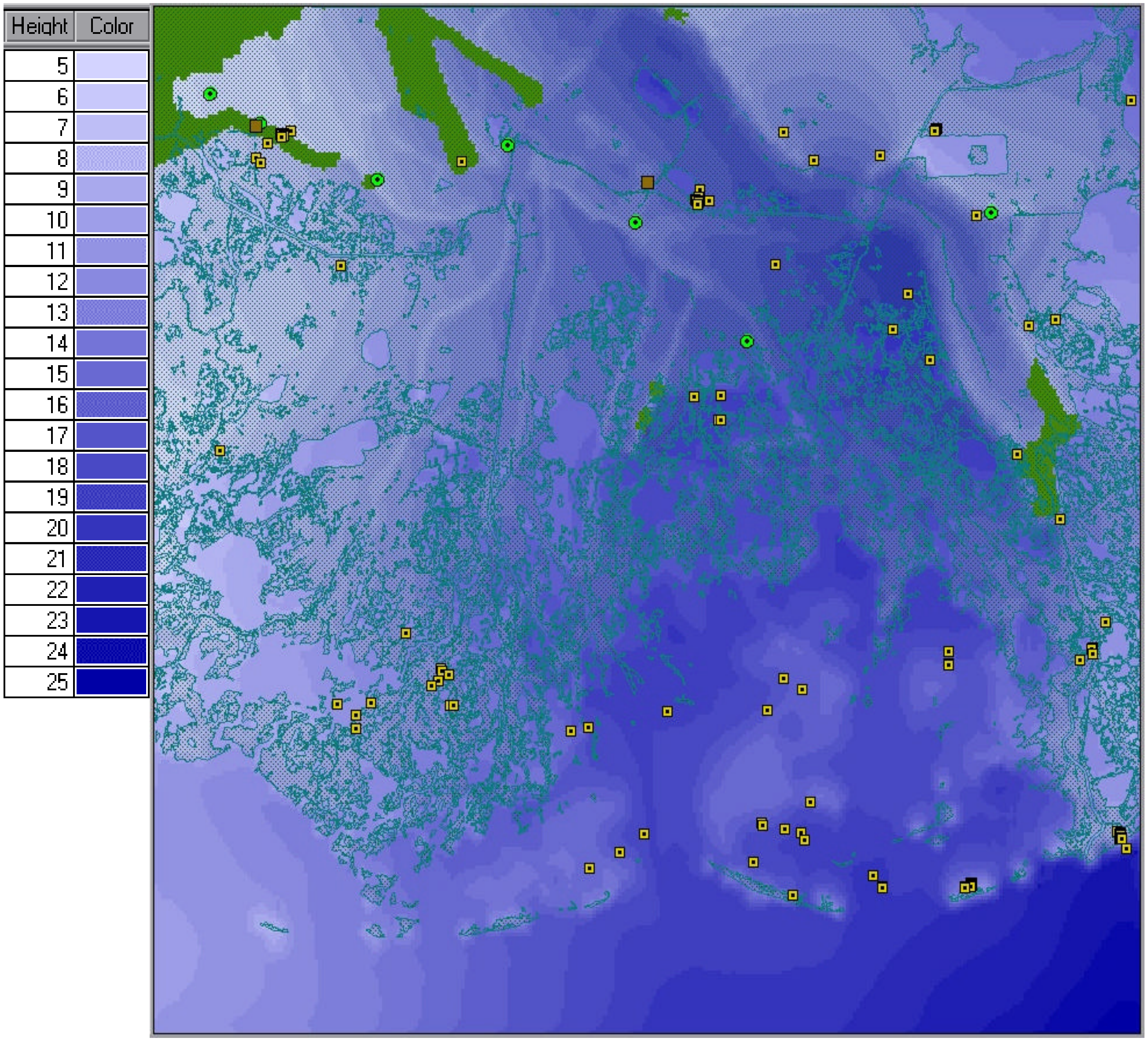

Figure 32. Distribution of crude petroleum and gas production facilities superimposed on the 1990's Maximum Storm Surge Elevation and Maximum Significant Wave Height composite.

available through an accompanying database file [pogxplmstamms] that can be linked to the structures. Full operator contact information may be linked from another included database file. Most of these structures are seaward of the immediate study area and are thus not included in the enumeration table.

Oil and Gas Structures

The distribution of oil and gas structures is shown in Figure 34. This is a point data set of the location of over 4,900 oil field platform structures and derricks in Louisiana coastal waters. John E. Chance & Associates, Inc acquired the geographic location coordinates on the platforms. Most of these platforms are associated with oil and gas wells from the Louisiana Department of Natural Resources data set. These points were used to geo-rectify the color IR digital orthophoto quarter quads (DOQQs) occurring over water. The platforms are visible in the images. Attributes include status and company.

Pipelines

This is a line data set for the location of pipelines (Figure 35). It is an incomplete data set because all the pipelines in the Louisiana coastal region have neither been located nor digitized. The data used in this study were acquired from the Louisiana Department of Natural Resources permit database, the Minerals Management Service, and the Louisiana Geological Survey. Attributes include: company, product code, type, status, burial information, size, length, origin, and destination. Attributes vary depending on source. Total pipeline miles in the study area is calculated at 5,033 with the layers used. This is an estimate only due to the fact that not all pipelines in the region have been documented, mapped, or digitized. Pipeline miles are not aggregated by wave/surge heights.

Composites and Other Layers

A composite of all of the above referenced layers is presented in Figure 36 where the combined surge and wave height trends are also illustrated. In Figure 37, the layers are shown relative to the change in combined storm surge levels and wave heights for the period 1950-1990's. The composite maps depicting all of the studied oil and gas layers in one view for both the maximums and the difference images show the strongly clustered distributions of most features around oil and gas fields and connected by pipelines. The figures dramatically illustrate the degree, extent, and complexity of the oil and gas infrastructure in Louisiana potentially exposed to storms. The map showing maximums dramatically illustrates the large clusters of oil and gas activity along the outer coastline exposed to the upper level of combined surge and wave heights, with these levels remaining strong in the center of the image in association with extensive infrastructure. The difference map illustrates some of the largest increase in heights occurring near some of the largest clusters of oil and gas facilities. The map also dramatically illustrates that nearly the entire infrastructure is potentially exposed to increased surge and wave heights over time.

Future studies could include many additional geo-spatial layers relative to the oil and gas infrastructure, hazardous waste facilities, roads and highways, power grid, population, and community facilities, to name a few examples.

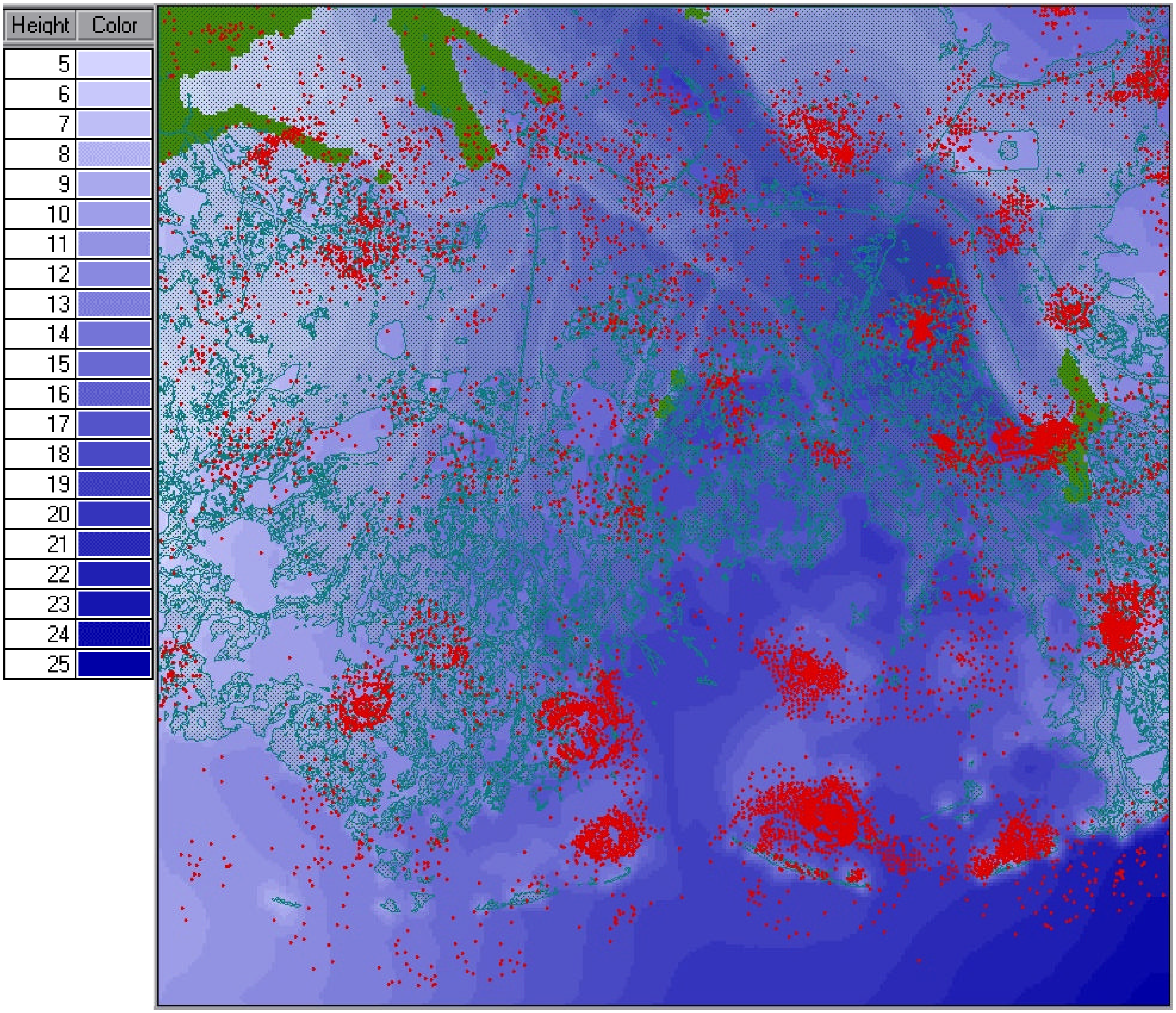

Figure 33. Distribution of oil and gas wells superimposed on the 1990's Maximum Storm Surge Elevation and Maximum Significant Wave Height composite.

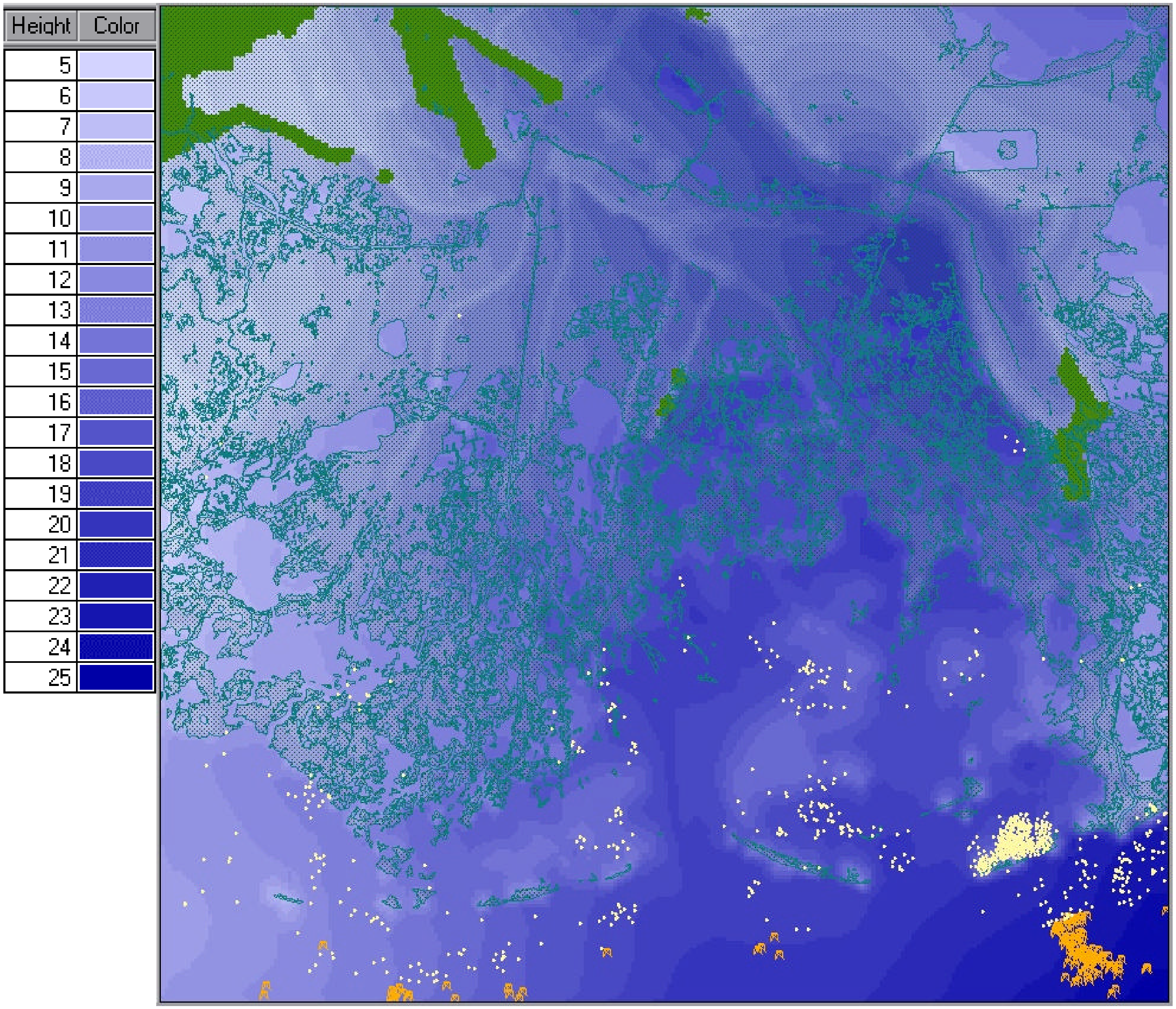

Figure 34. Distribution of platforms and structures superimposed on the 1990's Maximum Storm Surge Elevation and Maximum Significant Wave Height composite.

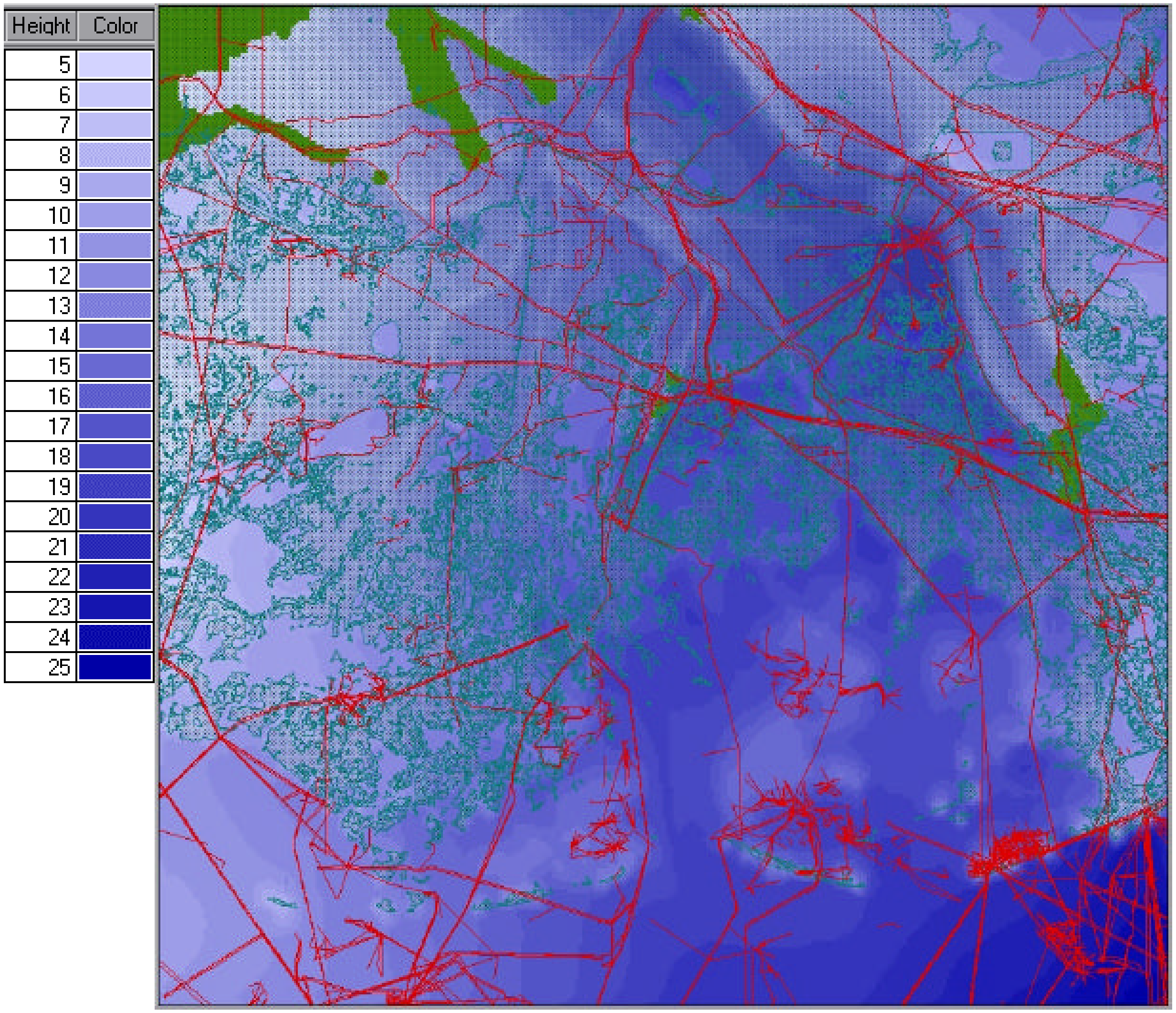

Figure 35. Distribution of pipelines superimposed on the 1990's Maximum Storm Surge Elevation and Maximum Significant Wave Height composite.

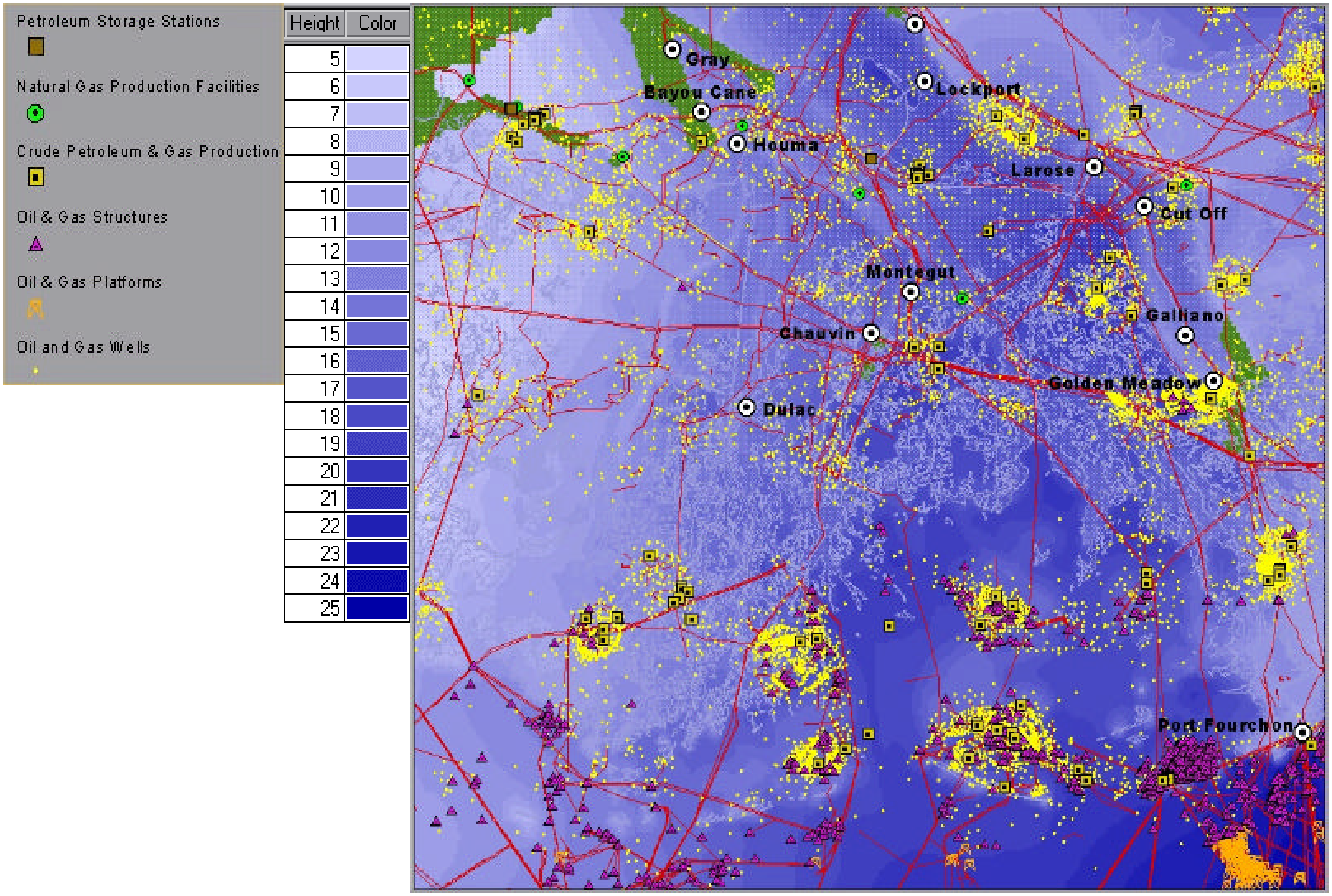

Figure 36. Distribution of crude petroleum and gas production facilities superimposed on the 1990's Maximum Storm Surge Elevation and Maximum Significant Wave Height composite.

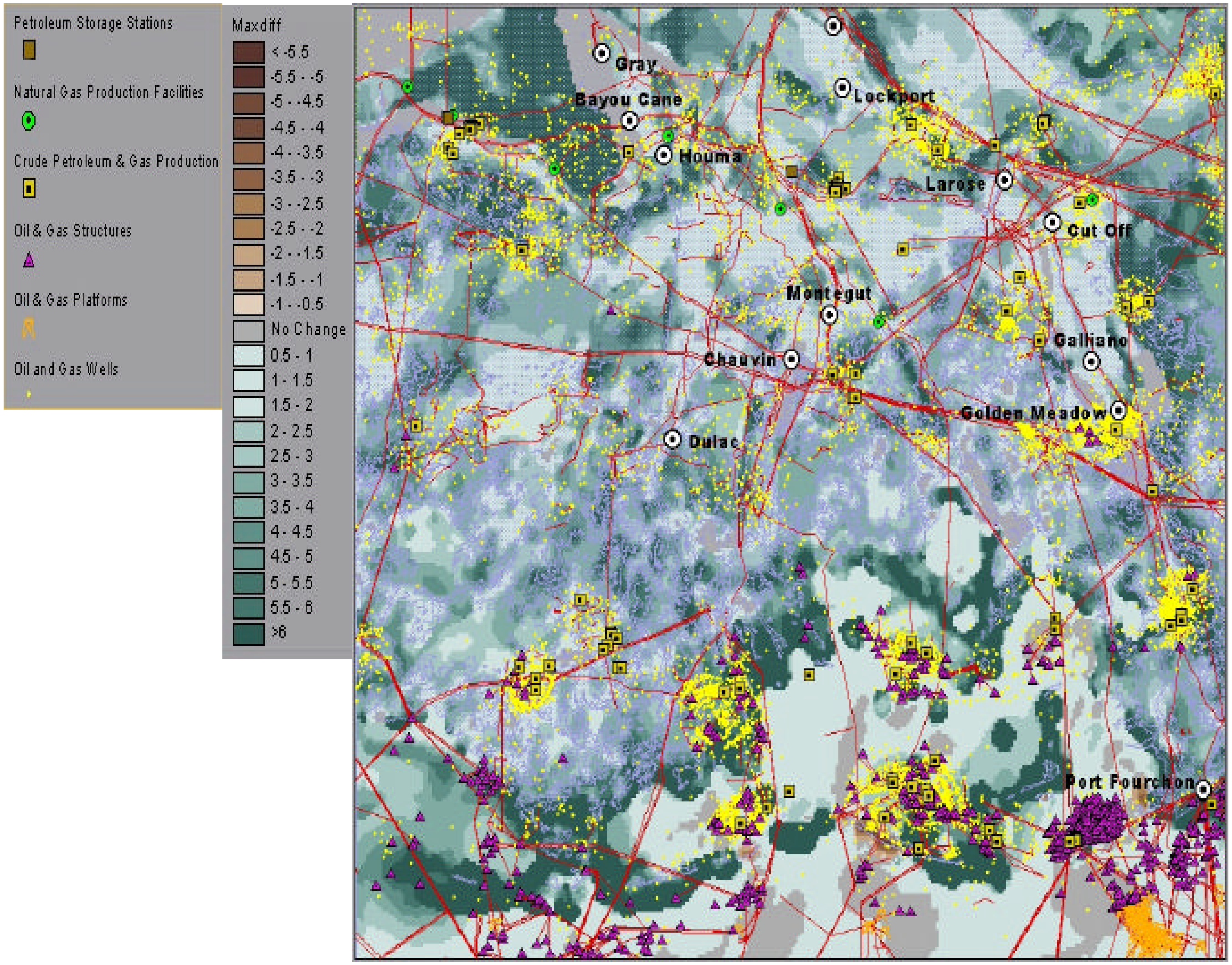

Figure 37. Distribution of wells, pipelines, structures, platforms and facilities superimposed on the change in combined storm surge levels and wave heights for the period 1950-1990's. The green shades indicate an increase in surge and wave height combined. Note that for clarity those increases above 6 ft are not provided. The reader is referred to Figure 24 for a more detailed representation of change.

SUMMARY and CONCLUSIONS

The potential impact of hurricane-generated storm surge and wave energy on the oil and gas infrastructure located in the study area is enormous and can be attributed to (1) the extent and number of facilities located there; and (2) the fact that barrier islands and marshes have drastically diminished in the past 40 years and are predicted to continue doing so in the absence of a major restoration effort.

Using a Hurricane Planetary Boundary model, a storm surge model (ADCIRC) and wave model (SWAN), the resultant data indicate that the vast majority of the study site underwent a considerable increase in combined surge and wave height during the interval 1950-1990's on running the "design" 1915 hurricane. This is an important period in time in that it represents the actual physical breakdown of the coast and to which the increase in surge and wave height can be directly attributed. Thus, the conclusion is important in that it demonstrates, for the first time, that the deterioration of the south-central Louisiana coast has likely resulted in an increase in surge and wave height during this period in time. The data from this current research suggest that the maximum difference in combined surge and waves occurs along the east flank of East Island showing an increase of 32 ft. This value is high because the east flank of the island migrated westward and land was transformed into water over the approximate 40 year period. Notably, the largest increases occur along the bay shorelines and barriers proper where land was transformed into water during the intervening time period. The magnitude of increase is typically 8-10 ft although change >12 ft is readily apparent along the marsh shorelines and barriers.

Over the approximate 30 year period between 1990's and 2020, the model forecast results also indicate that a significant increase in surge and wave height will occur throughout much of the study site. Increases are widespread in the study area with the largest occurring at Fourchon, Timbaliers and in particular, Isles Dernieres and the adjacent marshes. At these locations increasing values range from 10 to >12 ft. Throughout the marsh north of Terrebonne Bay, values increase from 6 ft, although in several location increases between 10 and >12 ft were computed.

Almost the entire study area experiences a significant increase in storm surge and wave inundation for the 70 year time difference (1950-2020). Virtually the entire barrier coast experiences an increase greater than 12 ft as does most of the fringing bay marsh. The interior of the marsh experiences typically 6-8 ft increases, although isolated areas experiencing >12 ft also occur.

The data presented here have very important implications for the oil and gas infrastructure located in the study site. The data suggest that in the absence of large-scale barrier and marsh restoration, the current infrastructure will experience increasing surge levels and increasing wave energy as the coast erodes. The data dramatically illustrate that nearly the entire infrastructure is potentially exposed to increased surge and wave heights over time. It also important to note that this conclusion pertains to tropical storms and weaker hurricanes that have shown historically, to have a high frequency of landfall along the Louisiana coast.

RECOMMENDED FUTURE WORK

This project was undertaken as a pilot effort to establish the linkage between coastal and wetland loss, storm surge and storm wave inundation, and variability with time and space. The data are conclusive in that they demonstrate the ability of barrier islands and coastal wetlands to mitigate surge and wave energy during tropical cyclones with a frequency of occurrence indicative of historical storms impacting the Louisiana coast. The data are extremely promising and the approach utilized here would yield very useful information if applied to other parts of the Louisiana coast, for example, east along the Barataria region and west along Vermillion parish. Additional "design" storms could be utilized and the research plan could be established in such a way as to assist in developing the optimum barrier island template (fill geometry) for future barrier island restoration.

A further recommendation involves the need for scientists and engineers to include numerical wave models in addition to surge simulations in all future efforts. As shown earlier in this report, omitting computations of wave heights from the approach severely underestimates the resultant super-elevated water level. Therefore, research efforts should be directed towards further developing integrated surge-current-wave models capable of simulating storm conditions in a more efficient manner. This would also assist in enhancing emergency preparedness by providing a very powerful tool which could enhance nowcast and forecast efforts.

ACKNOWLEDGEMENTS

We acknowledge the assistance provided by Drs. Lee Butler of Veri Tech. and Norm Scheffner of the Coastal and Hydraulics Laboratory, USACOE. Input was also provided by Secretary Jack Caldwell. This project was funded by the Louisiana Department of Natural Resources under contract #2503-02-35, the U.S. Minerals Management Service under contract #1435-01-99-CA-30951/85245 and the U.S. Geological Survey under contract #02CRAG0025.

REFERENCES

Barrier Island Feasibility Study, 1999. Louisiana Department of Natural Resources, Baton Rouge, LA.

Booij, N., R.C. Ris, and L.H. Holthuijsen, 1999. A third generation wave model for coastal regions: Part I: model description and validation, J. Geophys. Res., V104, 7649-7666.

Cardone, V.J., Greenwood, C.V., and Greenwood, J.A., 1992. "Unified Program for the Specification of Hurricane Boundary Layer Winds Over Surfaces of Specified Roughness," contract Report CERC-92-1, U.S. Army Engineer Waterways Experiment Station, Vicksburg, MS.

Coleman, J.M., Roberts, H.H. and Stone, G.W., 1998. Mississippi River Delta: An Overview *Journal of Coastal Research*, 14, 3, 698-717.

Gosselink, J. Coleman, J.M. and Stewart, R.E., 1998. Coastal Louisiana, in: Status and Trends of the Nation's Biological Resources, vol. 1, p. 385-436.

Penland, S., Suter, J.R., Sallenger, A.H., Williams, S.J., McBride, R.A. Westphal, K.E., Reimer, P.D. and Jaffe, B.E., 1989. Morphodynamic Signature of the 1985 Hurricane Impacts on the Northern Gulf of Mexico. Proc. Sixth Symposium on Coastal and Ocean Management (ASCE July 11-14, 1989, Charleston, South Carolina), pp. 4220-4233.

Jarvinen, B.R., Neumann, C.J., and Davis, M.A.S., 1988. "A Tropical Cyclone Data Tape for the North Atlantic Basin, 1886-1983: Contents, Limitations, and Uses," NOAA Technical Memorandum NWS NHC 22.

Jelesnianski, C.P. and Taylor, A..D., 1973. "A Preliminary View of Storm Surges Before and After Storm Modifications." NOAA Technical Memorandum ERL WMPO-3, Weather Modification Program Office, Bounder CO.

Mark, D. J., and Scheffner, N. W., 1997. "Coast of Delaware Hurricane Stage-Frequency Analysis," Miscellaneous Paper CHL-97-1, U.S. Army Engineer Waterways Experiment Station, Vicksburg, MS, January 1997.

Muller, R.A. and Stone, G.W., 2001. A Climatology of Tropical Storms and Hurricane Strikes to Enhance Vulnerability Predicition for the Southeast U.S. Coast. Journal of Coastal Research, 17, 4, 949-956.

McBride, R. A., Penland, S., Hiland, M. W., Williams, S. J., Westphal, K. A. Jaffe, B. E., and Sallenger, A. H., Jr., 1992, Analysis of barrier shoreline changes in Louisiana from 1853 to 1989, in Williams, S. J., Penland, Shea, and Sallenger, A. H., Jr., eds., Louisiana barrier island erosion study-atlas of barrier shoreline changes in Louisiana form 1853 to 1989: U.S. Geological Survey Miscellaneous Investigations Series I-2150-A, p. 36-97.

Resio, D. T., 1988. A steady-state wave model for coastal applications, Proc. 21-st Coast. Engrg, Conf. ASCE, 929-940.

Rogers, W.E., J.M. Kaihatu, N. Booij, L.H. Holthuijsen, 1999. Improving the numerics of a third generation wave action model. Naval Res. Lab. Rep. NRL/FR/7320-99-9695.

Scheffner, N.W., Mark, D.J., Blain, C.A., Westerink, J.J., and Luettich, R.A., 1994. "ADCIRC: An Advanced Three-Dimensional Circulation Model for Shelves, Coasts and Estuaries Report 5: A Tropical Storm Data Base for the East and Gulf of Mexico Coasts of the United States," Technical Report DRP-92-6, August 1994, U.S. Army Engineer Waterways Experiment Station, Vicksburg, MS.

Stone, G.W. and Finkl, C.W. (eds.), 1995. Impacts of Hurricane Andrew on the Coastal Zones of Florida and Louisiana: 22-26 August, 1992. *Journal of Coastal Research,* SI. 21, Coastal Education and Research Foundation, Fort Lauderdale, Fl., 364 pp.

Stone, G. W., Grymes, J., Steyer, K., Underwood, S., Robbins, K., and Muller, R. A., 1993. A Chronologic Overview of Climatological and Hydrological Aspects Associated with Hurricane Andrew and its Morphological Effects Along the Louisiana Coast, U.S.A. *Shore and Beach.* 61(2):2-12.

Stone, G. W., Xu, J.P. and Zhang, X.P, 1995. Estimation of the Wave Field During Hurricane Andrew and Morphological Impacts along the Louisiana Coast, *in* Impacts of Hurricane Andrew on the Coastal Zones of Florida and Louisiana: August 22-26, 1992. G. W. Stone and C. W. Finkl (eds.). *Journal Coastal Research Special Issue* 21, 234-253.

Stone, G.W., Grymes, J.M., Armbruster, C.A. and Huh, O.K., 1996 Overview and Impacts of Hurricane Opal on the Florida Coast." *EOS, Transactions of the American Geophysical Union,* 77551-553.

Stone, G.W., Grymes, J.M., Dingler, J.W. and Pepper, D.A., 1997. Overview and Significance of Hurricanes on the Louisiana Coast, USA. *Journal of Coastal Research,* 13, 3, 656-669.

Stone, G.W. and McBride, R.A., 1998. Louisiana barrier Islands and their Importance in Wetland Protection: Forecasting Shoreline Change and Subsequent Response of Wave Climate. *Journal of Coastal Research,* 14, 3, 900-916.

Stone, G.W., Wang, P., Pepper, D.A., Grymes, J.M., Roberts, H.H., Zhang, X.P., Hsu, S.A. and Huh, O.K., 1999. Researchers Begin to Unravel the Significance of Hurricanes on the Northern Gulf of Mexico Coast. *EOS, Transactions of the American Geophysical Union,*80, 27, 301-305.

Stone, G.W., Sheremet, A., Zhang, X., Walker, N.D., Grymes, J.M., Huh, O.K., Hsu, S.A., Blanchard, B., Bentley, S.J., 2003. A Decade of Tropical Cyclones in one Hurricane Season; Impacts of Isidore and Lili on the Louisiana Coast. (in prep.)

Tolman, H. L. , 1991. A third-generation model for wind waves on slowly varying, unsteady and inhomogeneous depths and currents. *Journal of Physical Oceanography*, 21, 782-797.

WAMDIG 1988: The WAM model - A third generation ocean wave prediction model. *Journal of Physical Oceanography*, 18, 1775-1810.